Published in final edited form as:
J Immunol. 2012 May 1; 188(9): 4278–4288. doi:10.4049/jimmunol.1101291.

IL-2 Simultaneously Expands Foxp3+ T Regulatory and T Effector Cells and Confers Resistance to Severe Tuberculosis (TB): Implicative Treg–T Effector Cooperation in Immunity to TB

Crystal Y. Chen[*,1], **Dan Huang**[*,1], **Shuyu Yao**[*], **Lisa Halliday**[†], **Gucheng Zeng**[*], **Richard C. Wang**[*], and **Zheng W. Chen**[*]

[*]Department of Microbiology and Immunology, Center for Primate Biomedical Research, College of Medicine, University of Illinois, Chicago, IL 60612

[†]Biological Research Labs, University of Illinois, Chicago, IL 60612

Abstract

The possibility that simultaneous expansion of T regulatory cells (Treg) and T effector cells early postinfection can confer some immunological benefits has not been studied. In this study, we tested the hypothesis that early, simultaneous cytokine expansion of Treg and T effector cells in a tissue infection site can allow these T cell populations to act in concert to control tissue inflammation/damage while containing infection. IL-2 treatments early after *Mycobacterium tuberculosis* infection of macaques induced simultaneous expansion of $CD4^+CD25^+Foxp3^+$ Treg, $CD8^+CD25^+Foxp3^+$ T cells, and $CD4^+$ T effector/$CD8^+$ T effector/$V\gamma2V\delta2$ T effector populations producing anti-*M. tuberculosis* cytokines IFN-γ and perforin, and conferred resistance to severe TB inflammation and lesions. IL-2–expanded $Foxp3^+$ Treg readily accumulated in pulmonary compartment, but despite this, rapid pulmonary trafficking/accumulation of IL-2–activated T effector populations still occurred. Such simultaneous recruitments of IL-2–expanded Treg and T effector populations to pulmonary compartment during *M. tuberculosis* infection correlated with IL-2–induced resistance to TB lesions without causing Treg-associated increases in *M. tuberculosis* burdens. In vivo depletion of IL-2–expanded $CD4^+Foxp3^+$ Treg and $CD4^+$ T effectors during IL-2 treatment of *M. tuberculosis*-infected macaques significantly reduced IL-2–induced resistance to TB lesions, suggesting that IL-2–expanded $CD4^+$ T effector cells and Treg contributed to anti-TB immunity. Thus, IL-2 can simultaneously activate and expand T effector cells and $Foxp3^+$ Treg populations and confer resistance to severe TB without enhancing *M. tuberculosis* infection.

Interleukin-2 is a T cell growth factor, predominantly activating cells expressing high-affinity IL-2R comprised of three chains, as follows: IL-2Rα(CD25), β(CD122), and γ(CD132) (1). Whereas $CD4^+CD25^+Foxp3^+$ T regulatory cells (Treg) constitutively express the high-affinity IL-2Rs and depend crucially on IL-2 for their growth and survival, activated T cells can also express IL-2R and proliferate in response to IL-2 (2, 3). Treg have been shown to suppress T cells and APC invitro (4), and invivo inhibit allograft rejection and autoimmune diseases (5, 6). Nevertheless, the role of Treg in infection and immunity remains less definite (4, 7). Some studies suggest that Treg suppress antimicrobial immune

Address correspondence to Dr. Zheng W. Chen, 909 S. Wolcott Avenue, MC790, Chicago, IL 60612. zchen@uic.edu.
[1]C.Y.C. and D.H. contributed equally to this work and share first authorship.

Disclosures
The authors have no financial conflicts of interest.

responses, leading to enhanced infection or persistence of pathogens (8–11). Other studies demonstrate that Foxp3$^+$ Treg facilitate, but do not suppress, antiviral immunity in mucosal interface (7). It is likely that cellular immunity against infections/diseases results from coordinated immune responses involving Foxp3$^+$ Treg and T effector cells. However, this compelling question is not formally addressed, and thus it is attractive to hypothesize that cytokine-activated Treg and T effector cells can act in concert to control tissue inflammation/damage and contain infection.

Tuberculosis (TB) remains one of the leading causes of global morbidity and mortality among infectious diseases largely due to HIV pandemics and multidrug-resistant TB. Precise elements of immunity during primary *Mycobacterium tuberculosis* infection of humans remain unknown, but might result from a tightly regulated balance of host responses and inflammatory processes. Although TB patients exhibit increased frequencies of Treg (12–15), it is not known whether such increases contribute to development of TB or result from increasing responses to inflammation or tissue damages. Because *M. tuberculosis* infection evolves TB granulomatous response or process in lungs, it is important to fully investigate pulmonary immune response and TB pathology. To date, whether Treg play a detrimental or protective role regarding TB inflammation or lesions has not been investigated at the pathology level, although adoptive transfer of Treg in mouse TB models can result in some increases in *M. tuberculosis* burden (16, 17).

Recent studies from us and others suggest that immune control of active *M. tuberculosis* infection is correlated with clonal expansion and efficient pulmonary recruiting of Ag-specific T effector cells (18, 19). However, it is not known whether these protective pulmonary T effector cell responses are indeed balanced or licensed by Treg. In fact, it remains unknown whether simultaneous expansion of Treg and protective T effector cells in pulmonary compartment can lead to favorable or detrimental disease outcome regarding TB inflammation and pathology. In this study, we conducted proof-of-concept studies in macaque TB models and determined whether simultaneous expansion of Treg and T effector cells by IL-2 treatments can allow these cell populations to act in concert to control TB inflammation and lung lesions without enhancing *M. tuberculosis* replication.

Materials and Methods

Macaque animals

A total of 34 cynomolgus monkeys, 4–8 y old, was used in the study. Animal studies were documented in animal protocols and approved by the Institutional Animal Care and Use Committee.

IL-2 treatment

Human rIL-2 (rhIL-2; Proleukin, Chiron, Emeryville, CA) was administered as we previously described (20). Briefly, 1.2 million IU human rIL-2 was given once daily for 5 d by s.c. injection in each cycle. The two-cycle intermittent IL-2 treatments started at days −3 and 15 postinfection. No detectable side effects were seen in IL-2–treated macaques. As controls, five animals received saline and four received BSA (27.2 μg) in 0.5 ml s.c. for 5 consecutive days. For the postinfection IL-2 treatment, IL-2 was given similarly for 5 d starting at day 15 after the infection.

M. tuberculosis infection

A total of 500 CFU *M. tuberculosis* Erdman was spread into bronchoalveolar interface of the right caudal (RC) lung lobe using bronchoscope-guided challenge technique, as we

described (21–23). This approach consistently induced severe TB in 100% of all 21 naive macaques that we tested (23–25).

Bronchoalveolar lavage

This was done as we previously described (21–23).

Isolation of single-cell suspensions and lymphocytes from blood and bronchoalveolar lavage fluid

These methods were described in detail in our recent publications (20, 21, 26). PBMC were isolated from freshly collected EDTA blood by Ficoll-Paque^{Plus} (Amersham, Piscataway, NJ) density gradient centrifugation. For isolation of lymphocytes from bronchoalveolar lavage (BAL) fluid, freshly retrieved BAL fluid was filtered through 40-μm cell strainers (BD Pharmingen) into 50-ml conical tubes (BD Pharmingen), followed by 5-min ×1500 rpm centrifugation. The supernatant was gently discarded without disturbing the cell pellets. Cell pellets were then treated with 5 ml RBC blood lysis buffer (Sigma-Aldrich) for 10 min or waited till the suspension became clear and washed once with 5% FBS-PBS.

Ags and Abs

The phosphoantigen compound, nonpeptidic phosphorylated metabolite of isoprenoid biosynthesis [e.g., (*E*)-4-hydroxy-3-methyl-but-2-enyl pyrophosphate (HMBPP)], specifically recognized by primate Vγ2Vδ2 T cells, but not by others, was produced, characterized, validated, and provided by H. Jomaa (Giessen, Germany). The purity of HMBPP was >98% (27). Purified protein derivative (PPD) and 15-mer overlapping peptides spanning Ag85B or ESAT6 were purchased from Mycos Research (Loveland, CO) and Gen-Script, respectively. Anti-CD28 (CD28.2; BD Pharmingen) and anti-CD49d (9F10; BD Pharmingen) were used in the assays as costimulatory Abs. The following mAbs were used for surface and intracellular cytokine staining for flow cytometry analyses: CD3 (SP34-2; BD Pharmingen), CD4 (L200; BD Pharmingen), CD8 (DK25; Dako), Vγ2 (7A5; Endogen), anti-Foxp3 Alexa Fluor 647 (259D; BioLegend; used for intracellular staining), IFN-γ allophycocyanin (4S.B3; BD Pharmingen), perforin-biotin (Pf-344; Mabtech, Cincinnati, OH); IL-17 PE (eBio64CAP17; eBioscience), streptavidin-Pacific blue (Invitrogen), and purified mouse IgG isotype control (eBioscience).

Immunofluorescent staining and flow cytometric analysis

Fluorescent Abs, including anti-Foxp3 Ab, immune staining of cell surface markers or intracellular Foxp3, and flow cytometry analyses were described in detail in our recent publications (20, 21, 26).

Detection of T effector cells using intracellular cytokine staining

Intracellular cytokine staining (ICS) was done, as previously described (20, 21, 26). A total of 10^5–10^6 BAL cells or 10^6 PBL plus mAbs CD28 (1 μg/ml) and CD49d (1 μg/ml) was incubated with Ag85B peptide pool (2 μg/ml), HMBPP (80 ng/ml), or media alone in 200 μl final volume for 1 h at 37°C, 5% CO_2, followed by an additional 5-h incubation in the presence of brefeldin A (GolgiPlug; BD). After staining cell surface CD3, CD4, CD8, or Vγ2 for 30 min, cells were permeabilized for 45 min (Cytofix/Cytoperm; BD) and stained for another 45 min to detect IFN-γ and perforin before resuspending in 2% formaldehyde-PBS.

Detection of Foxp3$^+$ cells

Five-color staining flow cytometry analysis was done, as we previously described (20), to measure frequencies of Foxp3$^+$ T cells. The panel for the staining was CD3/CD4/CD8/CD25/Foxp3.

CSFE-based proliferation assay for detection of Treg function

To assess Treg function, CD4$^+$CD25$^+$ T cells were isolated from PBL at week 3 using CD4$^+$CD25$^+$ Regulatory T Cell Isolation Kit for macaques (Miltenyi Biotec), as we previously described (20). CFSE-labeled PBMC were mixed at 2×10^5 cells/well with 0 or 1×10^5 PKH26-labeled CD4$^+$CD25$^+$ T cells in the presence or absence of PPD (15 μg/ml; Colorado Serum), HMBPP (40 ng/ml), and 5 μg/ml purified anti-human CD28 and anti-CD3 Abs (20). At days 7 or 8, cells were collected and stained with anti-Vδ2 or anti-Vγ2, anti-CD4, anti-CD8, and anti-CD3 Abs, as described above. Proliferation was analyzed by flow cytometry to determine the dilution of CFSE fluorescence intensity; the percentage of proliferation was calculated based on the number of CFSE^{dim} cells divided by the number of CFSE$^+$ cells (20).

Bacterial CFU counts

The methods were previously described (22, 24, 28). We followed the strategy, as recently described (22), to objectively measure CFU in lungs. Briefly, a half of cut sections of the RC lobe (the infection site), the right middle lobe, or the left caudal lobe from each animal was taken for CFU determination after the extensive gross pathologic evaluation was accomplished. If there were gross TB lesions in the respective lobe, a half of the lung tissue containing ~50% lesions was taken. If no visible lesions were seen in the respective lobe, a random half of tissue was taken for evaluation.

Gross pathologic analysis and the scoring system for TB lesions

Details were described in our previous publications (22). Briefly, animals were euthanized by i.v. barbiturate overdose, and immediately necropsied in a biological safety cabinet within a BSL-3 facility. Standard gross pathologic evaluation procedures were followed, with each step recorded and photographed at day 65 after *M. tuberculosis* infection. Lung lobes; bronchial, mesenteric, axillary, and inguinal lymph nodes; tonsils; and other major organs were collected and labeled. Multiple specimens from all tissues with gross lesions and remaining major organs were harvested. Gross observations including but not limited to the presence, location, size, number, and distribution of lesions were recorded. The scoring system (22, 29) was excised to calculate gross pathology scores for TB lesions in lungs infected by bronchoscope-guided inoculation. For each of lung lobes, granuloma prevalence was scored 0–4 for the following: 1) no visible granulomas; 2) 1–3 visible granulomas; 3) 4–10 visible granulomas; 4) >10 visible granulomas; and 5) miliary pattern of granulomas, respectively. Granuloma size was scored 0–3 for the following: 1) none present; 2) <1–2 mm; 3) 3–4 mm; and 4) >4 mm, respectively. Pulmonary consolidation or atelectasis as viewed from organ exterior and cut surfaces was scored 0–2 for the following: 1) absent; 2) present focally in one lobe; and 3) focally extensive within a lobe or involving multiple lobes. One score was also given for the presence of tuberculosis-related focal parietal pleural adhesions, pleural thickening and opacification, or pulmonary parenchymal cavitation. For hilar lymph nodes, enlargements were scored 0–3 for the following: 1) visible but not enlarged; 2) visibly enlarged unilaterally (≤2 cm); 3) visibly enlarged bilaterally (≤2 cm); and 4) visibly enlarged unilaterally or bilaterally >2 cm, respectively. Tuberculosis lesions in hilar lymph nodes were scored 0–4 for the following: 1) no granulomas visible on capsular or cut surface; 2) focal or multifocal, circumscribed, noncoalescing granulomas, <2 mm (≥nodes); 3) coalescing solid or caseating granulomas occupying <50% of nodal

architecture (≥nodes); 4) coalescing solid or caseating granulomas occupying >50% of nodal architecture, with residual nodal components still recognizable; and 5) complete granulomatous nodal effacement and caseation, respectively. One score was also given for tuberculosis-associated changes in other thoracic nodes. The tuberculosis lesions in each of the extrathoracic organs were scored similarly as each lung lobe. The pathology scoring of infected tissues was conducted in a blinded fashion.

Microscopic analysis of TB lesions

This was done, as we previously described (22, 24, 28). Briefly, the extent of involvement for each lung lobe was determined using digital scans to record total pixel counts on H&E-stained material and specimen area measured in square cm using Image-Pro Plus software (MediaCybernetics, Silver Spring, MD), as previously described (22, 24, 28). Granulomas were objectively compared for size, type (caseous, solid, suppurative, or mixed), distribution pattern (focal, multifocal, coalescing, and invasive), and cellular composition (absence or presence with degrees of lymphocytic cuff, mineralization, fibrosis, multinucleated giant cells, and epithelioid macrophages) between and within monkey groups.

Immunohistochemistry Foxp3 staining, as well as Foxp3 and CD4 costaining

Standard single-color immunohistochemistry protocol was used to stain Foxp3 in lung tissue sections and lymph node sections prepared from paraffin tissues. This was done essentially the same as we recently did (21, 24, 30), except that mouse anti-human Foxp3 mAb (BioLegend; clone 259D) was used in this study as the first Ab. The two-color Foxp3 and CD4 double staining in lung tissue and lymph node sections was done, as we previously described (30). Briefly, Foxp3 was stained as above, with diaminobenzidine as a substrate, followed by the Doublestain Block (Dako), and then stained for CD4 using rabbit anti-human CD4 (Lsbio; LS-B3426) and alkaline phosphatase polymer-conjugated goat anti-rabbit Igs (Dako). Fast red was used as a substrate. Staining colors were as follows: brown for Foxp3, red for CD4, and blue for nuclear.

Depleting anti-CD4 mAb administration

Depleting anti-CD4 mAb (OKT4-HuIgG; National Institutes of Health Nonhuman Primate Reagents Program) was i.v. administered to each of eight macaques at a dose of 50 mg/kg at days −5, 10, and 25, respectively, after *M. tuberculosis* infection.

Statistical analysis

The multivariate ANOVA and Student *t* test were used, as previously described (22, 30), to statistically analyze the data for differences between IL-2–treated and control groups.

Results

IL-2 treatments during *M. tuberculosis* infection of macaques induced increases in $CD4^+CD25^+Foxp3^+$ Treg in circulation and pulmonary compartment

We have recently shown that IL-2 treatment of bacillus Calmette-Guérin–infected macaques can induce expansion of $CD4^+CD25^+$ $Foxp3^+$ Treg in the blood (20). As initial efforts determining whether IL-2–expanded T effector cells and Treg can act in concert to control TB inflammation/lesions in lung tissues, macaques were treated intermittently with IL-2 regimen during pulmonary *M. tuberculosis* infection. The first IL-2 treatment was given daily for 5 d, initiating 3 d before *M. tuberculosis* infection (day −3); the second 5-d IL-2 treatment was given at day 15 after *M. tuberculosis* infection. As control, a group of macaques was similarly injected with saline or BSA. The intermittent IL-2 treatments reproducibly induced major expansion of $CD4^+CD25^+$ $Foxp3^+$ T cells in the macaques (Fig.

1A). Each cycle IL-2 treatment expanded $CD4^+CD25^+Foxp3^+$ T cells up to 25% of $CD4^+$ T cells (Fig. 1A), and to ~330 absolute Treg per μl blood (Fig. 1A). IL-2 treatment also induced expansion of $CD8^+CD25^+$ $Foxp3^+$ T cells (Fig. 1A, 1B).

Notably, intermittent IL-2 treatment regimen induced trafficking/accumulation of $CD4^+CD25^+Foxp3^+$ Treg and $CD8^+CD25^+Foxp3^+$ T cells in the pulmonary compartment as apparent increases in numbers of these cells were seen in the BAL fluid after each of the IL-2 treatments (Fig. 1B). The increases in Treg and T effectors in BAL fluid after the treatment consisted of increased accumulation of these T cells in lung tissues (30) (data not shown).

As demonstrated before (20), $CD4^+CD25^+$ T cells containing $Foxp3^+$ T cells after IL-2 treatment indeed inhibited immune responses of PPD-specific and HMBPP-specific T cells (Fig. 1C, 1D). Thus, intermittent IL-2 treatments during pulmonary *M. tuberculosis* infection expanded $CD4^+CD25^+Foxp3^+$ Treg in the circulation and pulmonary compartment.

Despite Treg expansion, $CD4^+$ T, $CD8^+$ T, and $V\gamma2V\delta2^+$ T effectors producing IFN-γ or perforin were still increased in blood and pulmonary compartment after IL-2 treatments

We have recently shown that rapid clonal expansion and pulmonary accumulation of $CD4^+$ and $CD8^+$ T effector cells producing IFN-γ correlate with vaccine-induced anti-TB immunity (19). Therefore, in this study, we sought to determine whether IL-2 treatments, although expanding Treg, also expand T effector cells and induce trafficking/accumulation of these T effectors in pulmonary compartment. Interestingly, despite Treg expansion, apparent increases in numbers of $CD4^+$ T, $CD8^+$ T, and $V\gamma2V\delta2$ T effector cells producing anti-TB cytokine IFN-γ or perforin (31, 32) after Ag stimulation were seen in the blood (Fig. 2A, 2B). These T effector populations were detected even without Ag stimulations using our modified ICS assay (Fig. 2A, 2C) (26, 33). There were similar increases in TNF-α–producing T cells (data not shown), but not IL-17–producing T cells (Fig. 2D). Furthermore, IL-2–expanded Treg did not appear to inhibit pulmonary migration of T effectors, as accumulation of $CD4^+$ T, $CD8^+$ T, and γδ T effector populations was detected in BAL fluid of the IL-2–treated macaques (Fig. 2A–C). Virtually, the IL-2–expanded T effector cells in pulmonary compartment peaked at the same time as did those IL-2–expanded $Foxp3^+$ Treg (Figs. 1, 2), suggesting that despite Treg expansion, T effector populations were still increased in blood and pulmonary compartment after IL-2 treatments.

IL-2 treatments, although expanding Treg and T effector populations, conferred resistance to TB inflammation and lesions

We then asked whether IL-2 treatments during *M. tuberculosis* infection would lead to Treg-associated suppression of anti-TB immunity or favorably confer a Treg-T effector–coordinated resistance to TB inflammation and lesions. Surprisingly, IL-2 treatments, although expanding Treg and T effector populations, led to apparent resistance to lung TB inflammation and lesions (Fig. 3A). The comparative efficacy evaluation at day 65 after *M. tuberculosis* infection demonstrated that control macaques treated with saline or BSA consistently showed severe TB lesions, characterized by caseation pneumonia or extensive coalescing granulomas at the RC (infection site) and other lung lobes as well as enlarged hilar lymph nodes with caseation (Fig. 3A, *upper panels*). In contrast, most IL-2–treated macaques showed focal or less-coalescing granulomas mostly limited to the RC lobe, without apparent occurrence of enlarged hilar lymph nodes (Fig. 3A). Gross TB granulomas or lesions were not seen at necropsy for one of nine IL-2–treated macaques. The digital microscopy screening of tissues from this animal revealed microscopy granulomas in the lung tissue sections from the RC lobe (Figs. 3A, 4). When gross pathology scores were

individually calculated (22) and statistically analyzed between IL-2–treated and control groups, the IL-treated group showed significantly milder gross TB pathology (Fig. 3B, $p < 0.01$).

Consistently, the histopathology evaluation demonstrated that the IL-2–treated group exhibited much milder TB lesions than the control group (Fig. 4). In the control group, most lung tissue sections showed widespread necrosis or TB pneumonia (Fig. 4). In contrast, most TB granulomas in the lung sections of the IL-2–treated group were well contained and highly lymphocytic, without extensive necrosis (Fig. 4). Immunohistochemistry analyses showed that $Foxp3^+CD4^+$ T cells were detectable in the small protective granulomas and hilar lymph nodes from IL-2–treated macaques even at the time the IL-2 treatment had ended for 45 d (*M. tuberculosis* endpoint was day 65) (Fig. 5). Control macaques appeared to exhibit few $Foxp3^+$ cells in nonprotective granulomas and hilar lymph nodes (Fig. 5).

Interestingly, in the presence of both Treg and T effector populations, we found no increases in *M. tuberculosis* replication in lung tissues (Figs. 2, 3C). The attenuation of TB pathology (Fig. 3A, 3B) coincided with the lower levels (without statistical significance) of *M. tuberculosis* CFU in lung tissue homogenates of IL-2–treated macaques compared with controls (Fig. 3C).

Thus, IL-2 treatments during early *M. tuberculosis* infection simultaneously expanded $Foxp3^+$ Treg and T effector populations, and conferred resistance to severe TB lesions.

Postinfection IL-2 treatment also induced major expansion of T effectors and $Foxp3^+$ Treg, and conferred resistance to severe TB lesions

The observation that intermittent IL-2 treatments at days −3 and 15 after *M. tuberculosis* infection could confer resistance to severe TB prompted us to determine whether postinfection IL-2 treatment at day 15 after pulmonary *M. tuberculosis* infection could also expand $Foxp3^+$ Treg and T effector cells, and confer resistance to TB lesions. Similarly, the postinfection IL-2 treatment simultaneously expanded $Foxp3^+$ Treg and T effector populations in blood and pulmonary compartment at day 5 after IL-2 treatment (day 20 after *M. tuberculosis* infection) (Fig. 6A). Such single IL-2 treatment still conferred resistance to TB lesions (Fig. 6B, 6C, $p < 0.05$), without Treg-associated increases in *M. tuberculosis* CFU in lungs (Fig. 6D).

In vivo depletion of IL-2–expanded $CD4^+Foxp3^+$ Treg and $CD4^+$ T effectors reduced, but did not eliminate IL-2–induced resistance to severe TB lesions

Because IL-2 expanded T effectors, Treg might not be the sole element for IL-2–induced resistance to TB lesions. We therefore sought to determine whether depleting $CD4^+$ T effectors and $Foxp3^+$ $CD4^+$ T cells could lead to changes in IL-2–induced resistance to TB lesions. We believed that depletion of $CD4^+$ T cells was the reasonable mechanistic experiment because of the following major reasons: 1) IL-2 treatment mostly expanded $CD4^+$ $Foxp3^+$ T cells and $CD4^+$ T effectors; 2) $CD4^+$ T cells play a major role in anti-*M. tuberculosis* infection (34); and 3) specific depletion of $Foxp3^+$ Treg in nonhuman primates is challenging because in vivo treatment of macaques with ONTAK immunotoxin only led to a partial reduction of $CD25^+$ T cells and $Foxp3^+$ T cells (35). Thus, two groups of macaques were depleted of $CD4^+$ T cells by administration of depleting anti-CD4 Ab, and then treated similarly with intermittent IL-2 regimen and saline (control), respectively, during early *M. tuberculosis* infection. IL-2–treated, CD4-depleted macaques were then evaluated for a loss or reduction of IL-2–induced resistance to severe TB. Treatments using depleting humanized OKT4A anti-CD4 Ab (36) efficiently depleted $CD4^+$ T cells in blood (Fig. 7A, *left*) and abrogated IL-2 expansion of $CD4^+CD25^+$ $Foxp3^+$ Treg (Fig. 7A, *middle/*

right) and $CD4^+$ T effector cells (Fig. 7B, *left*) during *M. tuberculosis* infection. IL-2 treatment of CD4-depleted macaques only expanded $CD8^+Foxp3^+$ T cells (Fig. 7A, *middle/right*) and to some extent $CD8^+$ Teffectors (Fig. 7B, *left*) and γδ T effectors, but not $CD4^+$ T cells (Fig. 7B, *right*). The macaques deleted of $CD4^+$ T cells during *M. tuberculosis* infection developed much worse TB lesions than those animals without CD4 depletion (Fig. 7C). Interestingly, IL-2–treated CD4-depleted macaques developed less severe TB lesions than saline-treated CD4-depleted animals, although there was no significant difference in *M. tuberculosis* burdens between these two CD4-depleted groups (Fig. 7C). Notably, IL-2–treated CD4-depleted macaques exhibited worse TB lesions than those IL-2–treated macaques without CD4 depletion (Fig. 7C), suggesting that IL-2–induced homeostatic protection against TB was significantly reduced by the depletion of IL-2–expanded $CD4^+Foxp3^+$ Treg and $CD4^+$ T effectors.

Discussion

We have made a novel discovery that IL-2 treatment in early-stage *M. tuberculosis* infection could simultaneously expand $Foxp3^+$ Treg and $CD4^+/CD8^+$/γδ T effector cells, and confer resistance to severe TB inflammation and lesions. Such homeostatic protection was not accompanied by Treg-associated increases in *M. tuberculosis* bacterial burdens. These findings suggest that simultaneous expansion of Treg and T effector cells allows these cell populations to act in concert to attenuate severe lung damages or lesions in infections. Our novel observations were made at pathology and immunology levels in the macaque TB model perhaps due to the fact that macaque TB models displayed more prominent human TB pathology than do mouse TB models (22).

IL-2 induced simultaneous transient expansion of $Foxp3^+$ Treg and Teffector cells during *M. tuberculosis* infection. Similar kinetics of IL-2 expansion of Treg and T effector cells were seen in the circulation and pulmonary compartment during the treatment. Given the possibility that before *M. tuberculosis* infection, low-level $CD4^+$ T, $CD8^+$ T, or γδ T effector cells may have been exposed to environmental nonpathogenic microbes, including nontuberculous mycobacteria, as described in humans (37), it would not be surprising that IL-2 treatments could expand $CD4^+/CD8^+$/γδ T effector cells producing IFN-γ and perforin. We also could not exclude the possibility that IL-2 treatments may enhance the ability of those non-Ag–specific αβ T/γδ T cells to proliferate and expand in response to in vitro *M. tuberculosis* Ag stimulation (potential bystander effects).

We did not see Treg-associated increases in *M. tuberculosis* burdens in lungs (20) during primary *M. tuberculosis* infection of macaques, despite simultaneous pulmonary accumulation of IL-2–expanded $Foxp3^+$ Treg and T effector cells. In the presence of both Treg and T effector cell populations, *M. tuberculosis* replication was not increased in lung tissues (Figs. 2, 3C). Virtually, coincident with the attenuation of TB (Fig. 3A, 3B) were the lower levels of *M. tuberculosis* CFU in lung tissue homogenates of IL-2–treated macaques compared with controls, although such decreases were not statistically significant (Fig. 3C).

IL-2–induced resistance to severe TB lesions might involve an optimal balance or cooperation between IL-2–expanded $CD4^+$ T effectors and Treg. Due to the lack of reagents specifically depleting $Foxp3^+$ T cells in macaques (35), we were not able to evaluate the relative importance of $Foxp3^+$ Treg versus $CD4^+/CD8^+$/γδ T effector cells. Nevertheless, our mechanistic studies depleting $CD4^+Foxp3^+$ Treg and $CD4^+$ T effector cells showed that a loss of these two $CD4^+$ T cell populations led to reduction in IL-2–induced resistance to TB lesions. IL-2–expanded Treg (20, 38, 39) may act as regulators downregulating *M. tuberculosis*-driven inflammation and lesions. IL-2–expanded $CD4^+$ T effectors producing anti-TB cytokines IFN-γ and perforin may also confer resistance to active *M. tuberculosis*

infection and TB lesions because $CD4^+$ T effector cells producing IFN-γ are crucial for anti-TB function in mice (18), HIV-1–infected humans (40), and SIV-infected macaques (41). The role of IL-2–expanded $CD8^+$ $Foxp3^+$ T cells, $CD8^+$ T effector cells, and Vγ2Vδ2 T effectors cannot be fully evaluated in the current study, although $CD8^+$ T cells can play a role in anti-TB immunity (22) and rapid recall-like expansion of Vγ2Vδ2 T cells can coincide with immunity against acutely fatal TB in juvenile rhesus macaques (42).

Rapid simultaneous recruitments of IL-2–expanded Treg and T effector cells to lungs during IL-2 treatment of early *M. tuberculosis* infection appear to be critical for mounting immune resistance to severe TB lesions in lungs. This is consistent with our recent observation that rapid clonal expansion and efficient pulmonary trafficking of Ag-specific T effector cells producing IFN-γ are one of the immune mechanisms underlying bacillus Calmette-Guérin vaccine-induced anti-TB immunity in macaques (19). It is important to note that whereas IL-2–expanded Treg can readily traffic to and accumulate in lungs, these Treg do not appear to suppress trafficking/accumulating of $CD4^+$, $CD8^+$, and γδ T effector cells in pulmonary compartment. Significant numbers of $Foxp3^+CD4^+$ T cells are still detected among the total $CD4^+$ T cell population in the TB granulomas of IL-2–treated macaques at the end point even though the IL-2 treatment stops 6 wk earlier (Fig. 5). This result and lung Treg function (Fig. 1D) implicate a reservation of $Foxp3^+CD4^+$ Treg histology and Treg function relevant to attenuation of TB lesion after they traffic to and accumulate in lung tissues. In fact, in patients with postprimary TB, TB damages in lung tissues appear to attract increases in Treg (43). In this study, in the macaque model of primary *M. tuberculosis* infection, simultaneous pulmonary accumulation of Treg and T effector cells during IL-2 treatments suggests that IL-2 may superimpose the cooperation between these cell populations balancing anti-TB immunity. Further studies appear to be justified to determine whether IL-2–induced cooperation between T effectors and Treg indeed delays pathology development or confers long-term benefits.

Our findings suggest that the benefit for IL-2 treatment of severe TB is to create an optimal balance between $Foxp3^+$ Treg and T effector cells. IL-2 treatment may provide efficient cytokine signaling for both $Foxp3^+$ Treg and activated T effectors that express high-affinity IL-2Rs. Such cosignaling effects would ensure simultaneous stimulation and expansion of $Foxp3^+$ Treg and T effectors. This may optimally develop a balance between $CD4^+$ $Foxp3^+$ Treg and $CD4^+$ T effector cells required for immune control of TB lesions or tissue damages because overwhelming dominance of Treg alone or T effectors alone may have harmful effects.

The IL-2–induced balance or cooperation between Treg and T effector cells may serve as a rationale for IL-2–based treatment of severe TB. This might indeed help to explain the IL-2–induced resistance to TB lesions without causing Treg-associated increases in *M. tuberculosis* burdens (16, 17). Our previous and current studies reproducibly demonstrate that pulmonary infection of naive macaques at a dose of ~500 CFU *M. tuberculosis* inevitably leads to high *M. tuberculosis* burden and severe TB lesions (23, 25, 33). High bacilli burden and severe TB lesions may result from overreacting inflammatory responses, because severe TB infection coincides with the inadequate overexpression of many immune molecules relevant to inflammation (21, 25). It is likely that rapidly expanded Treg during IL-2 treatments of the initial *M. tuberculosis* infection can downregulate the overreacting inflammatory responses and attenuate TB lesions. Such IL-2/Treg-driven control of TB lesions is indeed in line with a critical role for IL-2–expanded Treg in preventing mice from inflammatory diseases of autoimmunity (44). In contrast, IL-2–expanded T effector cells producing anti-TB cytokines IFN-γ and perforin may play a role in containing *M. tuberculosis* infection. The potential tissue damages caused by these T effector cells may be limited by IL-2–expanded Treg. The overacting Treg function might also be discounted by

Vγ2Vδ2 T effectors or other T effectors as activated Vγ2Vδ2 T effectors can antagonize the ability of IL-2 to over-expand Foxp3$^+$ Treg (20).

Thus, IL-2 treatments in early *M. tuberculosis* infection can simultaneously expand Foxp3$^+$ Treg and T effector populations in blood and pulmonary compartment, and conferred resistance to severe TB inflammation and lesions. The simultaneous pulmonary accumulation of IL-2–expanded Treg and T effector cells in early *M. tuberculosis* infection may be advantageous to single dominance of either Treg or T effectors, and somehow differs from simple Treg suppression of T cell responses as seen in lymphoid organs or in the in vitro assays. One study of rIL-2 adjunctive treatment in TB patients showed some effects (45), whereas another one reported a lack of IL-2–enhanced clearance of *M. tuberculosis* in TB drug-susceptible patients who received rIL-2 and four TB drugs (isoniazid, rifampin, pyrazinamide, and ethambutol) when compared to controls treated with the four TB drugs and placebo (46). The lack of IL-2–enhanced effects (46) might be due to the fact that the four anti-TB drugs overwhelmingly clear bacilli/TB and overshadow IL-2 benefits. The difference between human and macaque studies might be attributed to a number of factors, including stage or nature (postprimary versus primary TB) of *M. tuberculosis* infection, IL-2 dosing, and efficacy for expanding both T effectors and Treg. Thus, our novel findings in primary *M. tuberculosis* infection may hold the potential to apply IL-2–expanded Treg and T effector cells for fine-tuning host responses as immunotherapeutics against human TB or multidrug-resistant TB.

Acknowledgments

This work was supported by National Institutes of Health R01 Grants HL64560 and RR13601 (both to Z.W.C.).

We thank Dr. Keith Reimann for providing the depleting anti-CD4 mAb and other Chen laboratory staff for technical assistance.

Abbreviations used in this article

BAL	bronchoalveolar lavage
HMBPP	(*E*)-4-hydroxy-3-methyl-but-2-enyl pyrophosphate
ICS	intracellular cytokine staining
PPD	purified protein derivative
RC	right caudal
TB	tuberculosis
Treg	T regulatory cell

References

1. Taniguchi T, Minami Y. The IL-2/IL-2 receptor system: a current overview. Cell. 1993; 73:5–8. [PubMed: 8462103]
2. Hori S, Nomura T, Sakaguchi S. Control of regulatory T cell development by the transcription factor Foxp3. Science. 2003; 299:1057–1061. [PubMed: 12522256]
3. Fontenot JD, Gavin MA, Rudensky AY. Foxp3 programs the development and function of CD4+CD25+ regulatory T cells. Nat Immunol. 2003; 4:330–336. [PubMed: 12612578]
4. Shevach EM. Mechanisms of foxp3+ T regulatory cell-mediated suppression. Immunity. 2009; 30:636–645. [PubMed: 19464986]
5. Sakaguchi S. Naturally arising CD4+ regulatory T cells for immunologic self-tolerance and negative control of immune responses. Annu Rev Immunol. 2004; 22:531–562. [PubMed: 15032588]

6. Riley JL, June CH, Blazar BR. Human T regulatory cell therapy: take a billion or so and call me in the morning. Immunity. 2009; 30:656–665. [PubMed: 19464988]
7. Lund JM, Hsing L, Pham TT, Rudensky AY. Coordination of early protective immunity to viral infection by regulatory T cells. Science. 2008; 320:1220–1224. [PubMed: 18436744]
8. Belkaid Y, Rouse BT. Natural regulatory T cells in infectious disease. Nat Immunol. 2005; 6:353–360. [PubMed: 15785761]
9. Belkaid Y, Piccirillo CA, Mendez S, Shevach EM, Sacks DL. CD4+CD25+ regulatory T cells control *Leishmania major* persistence and immunity. Nature. 2002; 420:502–507. [PubMed: 12466842]
10. Scott-Browne JP, Shafiani S, Tucker-Heard G, Ishida-Tsubota K, Fontenot JD, Rudensky AY, Bevan MJ, Urdahl KB. Expansion and function of Foxp3-expressing T regulatory cells during tuberculosis. J Exp Med. 2007; 204:2159–2169. [PubMed: 17709423]
11. Zelinskyy G, Dietze K, Sparwasser T, Dittmer U. Regulatory T cells suppress antiviral immune responses and increase viral loads during acute infection with a lymphotropic retrovirus. PLoS Pathog. 2009; 5:e1000406. [PubMed: 19714239]
12. Garg A, Barnes PF, Roy S, Quiroga MF, Wu S, García VE, Krutzik SR, Weis SE, Vankayalapati R. Mannose-capped lipoarabinomannan-and prostaglandin E2-dependent expansion of regulatory T cells in human *Mycobacterium tuberculosis* infection. Eur J Immunol. 2008; 38:459–469. [PubMed: 18203140]
13. Li L, Lao SH, Wu CY. Increased frequency of CD4(+)CD25 (high) Treg cells inhibit BCG-specific induction of IFN-gamma by CD4(+) T cells from TB patients. Tuberculosis. 2007; 87:526–534. [PubMed: 17851131]
14. Sharma PK, Saha PK, Singh A, Sharma SK, Ghosh B, Mitra DK. FoxP3+ regulatory T cells suppress effector T-cell function at pathologic site in miliary tuberculosis. Am J Respir Crit Care Med. 2009; 179:1061–1070. [PubMed: 19246720]
15. Geffner L, Yokobori N, Basile J, Schierloh P, Balboa L, Romero MM, Ritacco V, Vescovo M, González Montaner P, Lopez B, et al. Patients with multidrug-resistant tuberculosis display impaired Th1 responses and enhanced regulatory T-cell levels in response to an outbreak of multidrug-resistant *Mycobacterium tuberculosis* M and Ra strains. Infect Immun. 2009; 77:5025–5034. [PubMed: 19720756]
16. Kursar M, Koch M, Mittrücker HW, Nouailles G, Bonhagen K, Kamradt T, Kaufmann SH. Cutting edge: regulatory T cells prevent efficient clearance of *Mycobacterium tuberculosis*. J Immunol. 2007; 178:2661–2665. [PubMed: 17312107]
17. Shafiani S, Tucker-Heard G, Kariyone A, Takatsu K, Urdahl KB. Pathogen-specific regulatory T cells delay the arrival of effector T cells in the lung during early tuberculosis. J Exp Med. 2010; 207:1409–1420. [PubMed: 20547826]
18. Cooper AM. Cell-mediated immune responses in tuberculosis. Annu Rev Immunol. 2009; 27:393–422. [PubMed: 19302046]
19. Du G, Chen CY, Shen Y, Qiu L, Huang D, Wang R, Chen ZW. TCR repertoire, clonal dominance, and pulmonary trafficking of *Mycobacterium*-specific CD4+ and CD8+ T effector cells in immunity against tuberculosis. J Immunol. 2010; 185:3940–3947. [PubMed: 20805423]
20. Gong G, Shao L, Wang Y, Chen CY, Huang D, Yao S, Zhan X, Sicard H, Wang R, Chen ZW. Phosphoantigen-activated V gamma 2V delta 2 T cells antagonize IL-2-induced CD4+CD25+Foxp3+ T regulatory cells in mycobacterial infection. Blood. 2009; 113:837–845. [PubMed: 18981295]
21. Yao S, Huang D, Chen CY, Halliday L, Zeng G, Wang RC, Chen ZW. Differentiation, distribution and gammadelta T cell-driven regulation of IL-22-producing T cells in tuberculosis. PLoS Pathog. 2010; 6:e1000789. [PubMed: 20195465]
22. Chen CY, Huang D, Wang RC, Shen L, Zeng G, Yao S, Shen Y, Halliday L, Fortman J, McAllister M, et al. A critical role for CD8 T cells in a nonhuman primate model of tuberculosis. PLoS Pathog. 2009; 5:e1000392. [PubMed: 19381260]
23. Wei H, Wang R, Yuan Z, Chen CY, Huang D, Halliday L, Zhong W, Zeng G, Shen Y, Shen L, et al. DR*W201/P65 tetramer visualization of epitope-specific CD4 T-cell during *M. tuberculosis*

infection and its resting memory pool after BCG vaccination. PLoS One. 2009; 4:e6905. [PubMed: 19730727]

24. Huang D, Shen Y, Qiu L, Chen CY, Shen L, Estep J, Hunt R, Vasconcelos D, Du G, Aye P, et al. Immune distribution and localization of phosphoantigen-specific Vgamma2Vdelta2 T cells in lymphoid and nonlymphoid tissues in *Mycobacterium tuberculosis* infection. Infect Immun. 2008; 76:426–436. [PubMed: 17923514]
25. Qiu L, Huang D, Chen CY, Wang R, Shen L, Shen Y, Hunt R, Estep J, Haynes BF, Jacobs WR Jr, et al. Severe tuberculosis induces unbalanced up-regulation of gene networks and overexpression of IL-22, MIP-1alpha, CCL27, IP-10, CCR4, CCR5, CXCR3, PD1, PDL2, IL-3, IFN-beta, TIM1, and TLR2 but low antigen-specific cellular responses. J Infect Dis. 2008; 198:1514–1519. [PubMed: 18811584]
26. Ali Z, Yan L, Plagman N, Reichenberg A, Hintz M, Jomaa H, Villinger F, Chen ZW. Gammadelta T cell immune manipulation during chronic phase of simian HIV infection confers immunological benefits. J Immunol. 2009; 183:5407–5417. [PubMed: 19786533]
27. Ali Z, Shao L, Halliday L, Reichenberg A, Hintz M, Jomaa H, Chen ZW. Prolonged (E)-4-hydroxy-3-methyl-but-2-enyl pyrophosphate-driven antimicrobial and cytotoxic responses of pulmonary and systemic Vgamma2Vdelta2 T cells in macaques. J Immunol. 2007; 179:8287–8296. [PubMed: 18056373]
28. Larsen MH, Biermann K, Chen B, Hsu T, Sambandamurthy VK, Lackner AA, Aye PP, Didier P, Huang D, Shao L, et al. Efficacy and safety of live attenuated persistent and rapidly cleared *Mycobacterium tuberculosis* vaccine candidates in non-human primates. Vaccine. 2009; 27:4709–4717. [PubMed: 19500524]
29. Lin PL, Pawar S, Myers A, Pegu A, Fuhrman C, Reinhart TA, Capuano SV, Klein E, Flynn JL. Early events in *Mycobacterium tuberculosis* infection in cynomolgus macaques. Infect Immun. 2006; 74:3790–3803. [PubMed: 16790751]
30. Huang D, Chen CY, Ali Z, Shao L, Shen L, Lockman HA, Barnewall RE, Sabourin C, Eestep J, Reichenberg A, et al. Antigen-specific Vgamma2Vdelta2 T effector cells confer homeostatic protection against pneumonic plaque lesions. Proc Natl Acad Sci USA. 2009; 106:7553–7558. [PubMed: 19383786]
31. Cooper AM, Khader SA. The role of cytokines in the initiation, expansion, and control of cellular immunity to tuberculosis. Immunol Rev. 2008; 226:191–204. [PubMed: 19161425]
32. Woodworth JS, Wu Y, Behar SM. *Mycobacterium tuberculosis*-specific CD8+ T cells require perforin to kill target cells and provide protection in vivo. J Immunol. 2008; 181:8595–8603. [PubMed: 19050279]
33. Yao S, Huang D, Chen CY, Halliday L, Zeng G, Wang RC, Chen ZW. Differentiation, distribution and gammadelta T cell-driven regulation of IL-22-producing T cells in tuberculosis. PLoS Pathog. 2010; 6:e1000789. [PubMed: 20195465]
34. Mogues T, Goodrich ME, Ryan L, LaCourse R, North RJ. The relative importance of T cell subsets in immunity and immunopathology of airborne *Mycobacterium tuberculosis* infection in mice. J Exp Med. 2001; 193:271–280. [PubMed: 11157048]
35. Pandrea I, Gaufin T, Brenchley JM, Gautam R, Monjure C, Gautam A, Coleman C, Lackner AA, Ribeiro RM, Douek DC, Apetrei C. Cutting edge: experimentally induced immune activation in natural hosts of simian immunodeficiency virus induces significant increases in viral replication and CD4+ T cell depletion. J Immunol. 2008; 181:6687–6691. [PubMed: 18981083]
36. Edghill-Smith Y, Golding H, Manischewitz J, King LR, Scott D, Bray M, Nalca A, Hooper JW, Whitehouse CA, Schmitz JE, et al. Smallpox vaccine-induced antibodies are necessary and sufficient for protection against monkeypox virus. Nat Med. 2005; 11:740–747. [PubMed: 15951823]
37. Brown-Elliott BA, Griffith DE, Wallace RJ Jr. Newly described or emerging human species of nontuberculous mycobacteria. Infect Dis Clin North Am. 2002; 16:187–220. [PubMed: 11917813]
38. Weiss L, Letimier FA, Carriere M, Maiella S, Donkova-Petrini V, Targat B, Benecke A, Rogge L, Levy Y. In vivo expansion of naive and activated CD4+CD25+FOXP3+ regulatory T cell populations in interleukin-2-treated HIV patients. Proc Natl Acad Sci USA. 2010; 107:10632–10637. [PubMed: 20498045]

39. Sereti I, Imamichi H, Natarajan V, Imamichi T, Ramchandani MS, Badralmaa Y, Berg SC, Metcalf JA, Hahn BK, Shen JM, et al. In vivo expansion of CD4CD45RO-CD25 T cells expressing foxP3 in IL-2-treated HIV-infected patients. J Clin Invest. 2005; 115:1839–1847. [PubMed: 15937547]
40. Boom WH, Canaday DH, Fulton SA, Gehring AJ, Rojas RE, Torres M. Human immunity to *M. tuberculosis*: T cell subsets and antigen processing. Tuberculosis. 2003; 83:98–106. [PubMed: 12758197]
41. Chen ZW. Immunology of AIDS virus and mycobacterial co-infection. Curr HIV Res. 2004; 2:351–355. [PubMed: 15544456]
42. Shen Y, Zhou D, Qiu L, Lai X, Simon M, Shen L, Kou Z, Wang Q, Jiang L, Estep J, et al. Adaptive immune response of Vgamma2Vdelta2+ T cells during mycobacterial infections. Science. 2002; 295:2255–2258. [PubMed: 11910108]
43. Welsh KJ, Risin SA, Actor JK, Hunter RL. Immunopathology of postprimary tuberculosis: increased T-regulatory cells and DEC-205-positive foamy macrophages in cavitary lesions. Clin Dev Immunol. 2011; 2011:307631. [PubMed: 21197439]
44. Webster KE, Walters S, Kohler RE, Mrkvan T, Boyman O, Surh CD, Grey ST, Sprent J. In vivo expansion of T reg cells with IL-2-mAb complexes: induction of resistance to EAE and long-term acceptance of islet allografts without immunosuppression. J Exp Med. 2009; 206:751–760. [PubMed: 19332874]
45. Johnson BJ, Bekker LG, Rickman R, Brown S, Lesser M, Ress S, Willcox P, Steyn L, Kaplan G. rhuIL-2 adjunctive therapy in multidrug resistant tuberculosis: a comparison of two treatment regimens and placebo. Tuber Lung Dis. 1997; 78:195–203. [PubMed: 9713652]
46. Johnson JL, Ssekasanvu E, Okwera A, Mayanja H, Hirsch CS, Nakibali JG, Jankus DD, Eisenach KD, Boom WH, Ellner JJ, Mugerwa RD. Uganda-Case Western Reserve University Research Collaboration. Randomized trial of adjunctive interleukin-2 in adults with pulmonary tuberculosis. Am J Respir Crit Care Med. 2003; 168:185–191. [PubMed: 12702550]

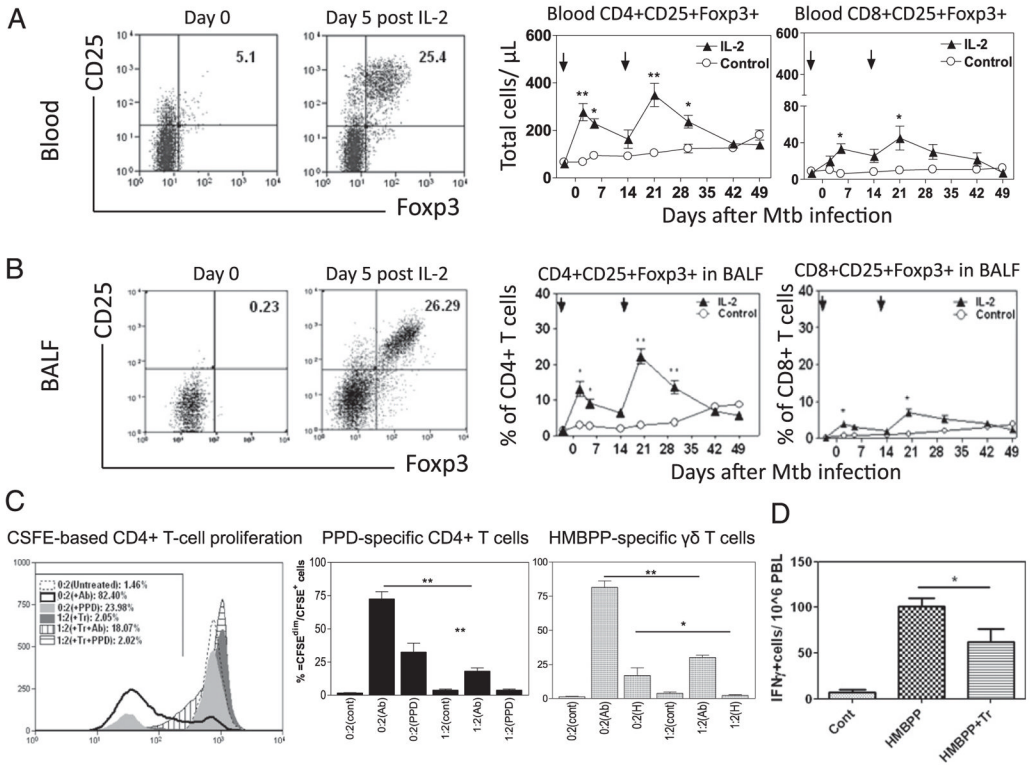

FIGURE 1.

Intermittent 5-d IL-2 treatments starting at days −3 and 15 (pointed by arrows) after *M. tuberculosis* infection induce major transient expansion of $CD4^+CD25^+Foxp3^+$ Treg and $CD8^+CD25^+Foxp3^+$ T cells. (**A**) Representative flow cytometry histograms gated on CD4 (*left*) and graph data (*middle* and *right*) of absolute numbers of $CD4^+CD25^+Foxp3^+$ T cells and $CD8^+CD25^+Foxp3^+$ T cells, respectively, in the blood. Graph data are means with SEM from six macaques/group. $^{**}p < 0.01$, $^{*}p < 0.05$. Noninfected macaques exhibited similar increases in Treg in pulmonary compartments after IL-2 treatment (data not shown). (**B**) BAL fluid (BALF) data in a similar fashion as (A), except that numbers in graphs (*middle* and *right*) are percentages of $CD4^+$ or $CD8^+$ T cells ($n = 6$). Increases in $Foxp3^+$ cells in BALF corresponded to accumulation of them in lung tissues of treated macaques (data not shown). (**C**) Purified $CD4^+CD25^+$ T cells inhibited PPD-stimulated $CD4^+$ T cell proliferation and HMBPP-stimulated γδ T cell proliferation. Approximately 87% of purified $CD4^+CD25^+$ T cells expressed Foxp3. *Left panel*, Representative flow cytometry histograms for the data from CFSE-based proliferation assay, with percentage numbers of proliferating cells (left-shifting $CSFE^{dim}$ cells) indicated. The 0:2(+Ab) or 1:2(Tr^+ Ab) ratio indicated that 0 or 1×10^5 $CD4^+CD25^+$ T cells (Tr) were incubated with 2×10^5 PBL of IL-2–treated macaques in the presence of anti-CD3/anti-CD28 Ab, whereas the 0:2(+PPD) or 1:2(Tr^+ PPD) ratio denoted that 0 or 1×10^5 Tr were incubated with 2×10^5 PBL of IL-2–treated macaques in the presence of PPD (see *Materials and Methods*). The *middle two bar panels* show the $Foxp3^+$ cell-driven suppression of PPD-specific T cell proliferation and HMBPP(H)-specific γδ T cell proliferation, respectively. The 0:2(PPD) or 1:2(PPD) ratio indicates that 0 or 1×10^5 Tr were incubated with 2×10^5 PBL of IL-2–treated macaques ($n = 5$) in each of five wells in the presence of PPD, with anti-CD3/anti-CD28 Ab as positive control (see *Materials and Methods*). The 0:2(H) or 1:2(H) ratio denotes 0 or 1×10^5 Tr mixed with 2×10^5 PBL containing γδ T cells in presence of HMBPP. (**D**) $CD4^+CD25^+$ T cells purified from BAL cells at day 5 after IL-2 treatment suppressed HMBPP-driven

production of IFN-γ by autologous γδ T cells in PBL. $CD4^+CD25^+$(Tr):PBL ratio was 1:2, $n = 4$. Assay was done as previously described (24).

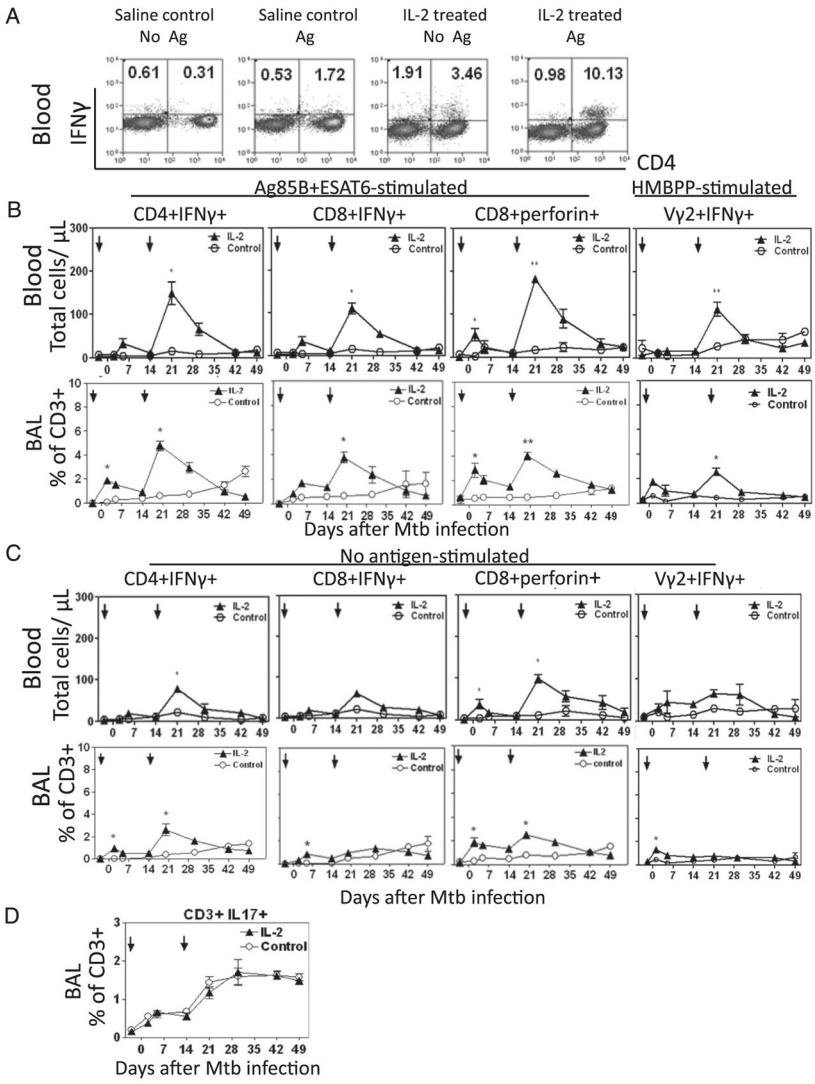

FIGURE 2.

Despite Treg expansion, $CD4^+$ T, $CD8^+$ T, and γδ T effectors were still increased in blood and pulmonary compartment after intermittent 5-d IL-2 treatments during *M. tuberculosis* infection. (**A**) Representative cytometry histograms of T effector cells measured by ICS with or without Ag stimulation at day 5 after the second IL-2 or saline treatment (day 20 after *M. tuberculosis* infection). (**B**) Compares effector cells detected by ICS after in vitro stimulation with pooled Ag85B and ESAT6 peptides, and HMBPP (for $V\gamma2V\delta2^+$ T effectors), respectively. $n = 6$/group. $^*p < 0.05$ and $^{**}p < 0.01$, respectively, for comparisons between IL-2–treated and control groups. (**C**) Frequencies of $CD8^+$, $CD4^+$, and $V\gamma2V\delta2^+$ T effector cells measured by ICS without Ag stimulation between the control and IL-2–treated groups are compared. $n = 6$/group. (**D**) Frequencies of blood T effector cells producing IL-17 after in vitro Ag85B/ESAT6 stimulation between the control and IL-2–treated groups are compared. $n = 5$.

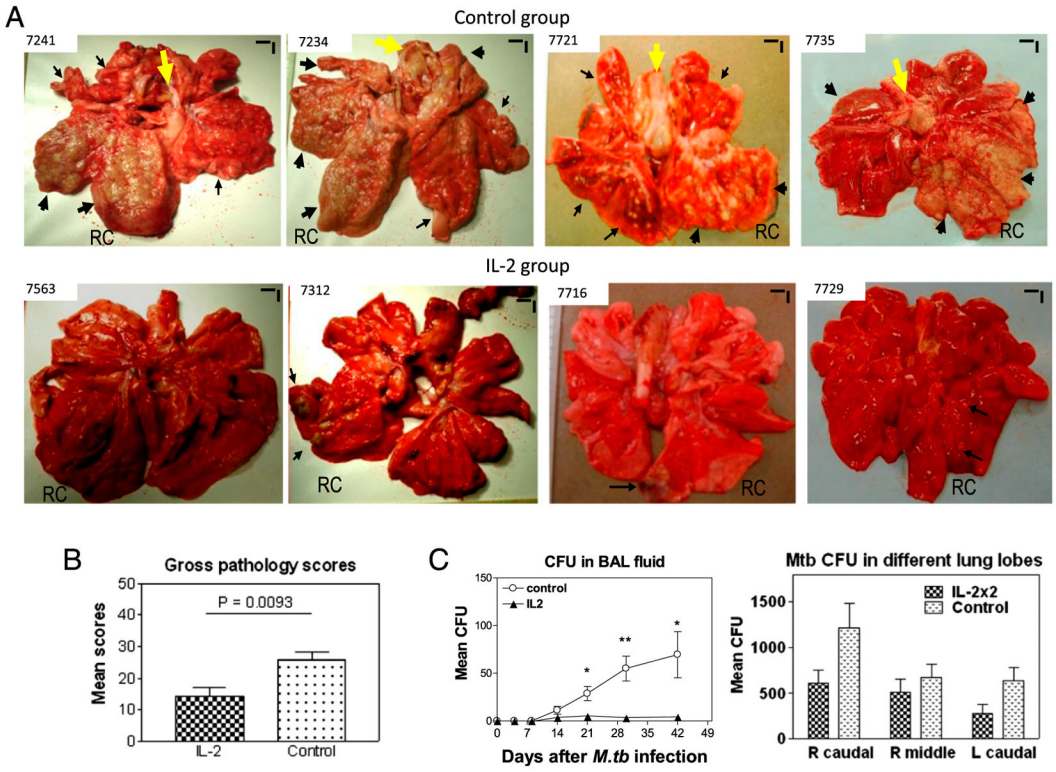

FIGURE 3.

IL-2 treatments during early *M. tuberculosis* infection, while expanding Treg and T effectors, surprisingly conferred resistance to severe TB lesions, without causing Treg-associated increases in *M. tuberculosis* bacterial burdens. (**A**) Digital photos of cut sections of lung lobes from 8 representatives of 18 macaques (9 IL-2 treated and 9 controls treated with saline or BSA). Lungs and other organs were obtained in complete necropsy at day 65 after *M. tuberculosis* infection. Macaque ID numbers are shown in *upper left corners*, with the RC lobe (infection site) indicated in each photo. Extent and severity of the lesions could be adjudged based on the examples pointed by large arrows for caseation pneumonia or extensive coalescing granulomas and by small arrows for less coalescing or small granulomas. Yellow arrows indicate the enlarged hilar lymph nodes with caseation. Note that the IL-2–treated macaque ID 7563 did not show any detectable gross TB lesions, although small microscopic granulomas were detected in histology sections of the RC lobe. Additional 5 IL-2–treated macaques displayed focal or less-coalescing granulomas mostly limited to the RC lobe, without apparent occurrence of enlarged hilar lymph nodes. Small vertical/horizontal bars at *upper right corner* of each photo represent the 1-cm scale derived from the fluorescence rulers of original photos. Greater than 50% of controls versus 10% of IL-2–treated macaques had extrathoracic TB dissemination. The efficacy evaluation was done sequentially in three separate trials using a total of 18 macaques. (**B**) Mean gross pathology scores for IL-2–treated and control groups. The scores were calculated and compared, as we previously described (22). (**C**) Simultaneous expansion of Foxp3$^+$ Treg and T effector populations did not result in Treg-associated increases in bacterial burdens in lungs. Shown are mean CFU counts in BAL fluid over time before the end time point (*left*) and in lung tissue homogenates (*right*) of different lung lobes collected at the end point from IL-2–treated and control groups. A total of 10 ml BAL fluid/cells and 10 ml lung tissue homogenates was used for CFU enumeration, respectively. The significantly higher *M. tuberculosis* CFU in BAL fluid were seen in the control group (C, *left*), and this might be

due to the fact that TB necrosis process was taking place and releasing more bacterial organisms into the airway over time before the end point. $p < 0.05$ for comparisons in BAL at weeks 3–6; $p > 0.05$ for comparisons of CFU counts in tissue homogenates of RC, right middle, and left caudal lung lobes between the IL-2–treated and control groups. $n = 9$/group. *$p < 0.05$, **$p < 0.01$.

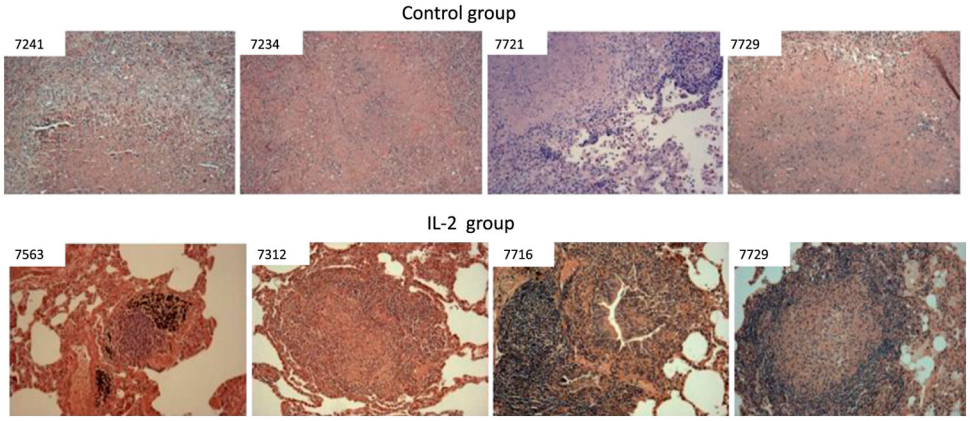

FIGURE 4.

TB granulomas in IL-2–treated group were less necrotic than those in controls. Histopathology analyses show that control macaques exhibited widespread necrosis, fulminant TB pneumonia, and TB hemorrhage/thrombosis lesions. The alveolar septa are destroyed or indistinct. In contrast, most TB granulomas in lung sections of the IL-2–treated group were well contained and lymphocytic (note the lymphocyte cuff), without widespread necrosis. Original magnification ×100 for all photos. Similar contrasting data were also seen in other controls and IL-2–treated macaques, respectively.

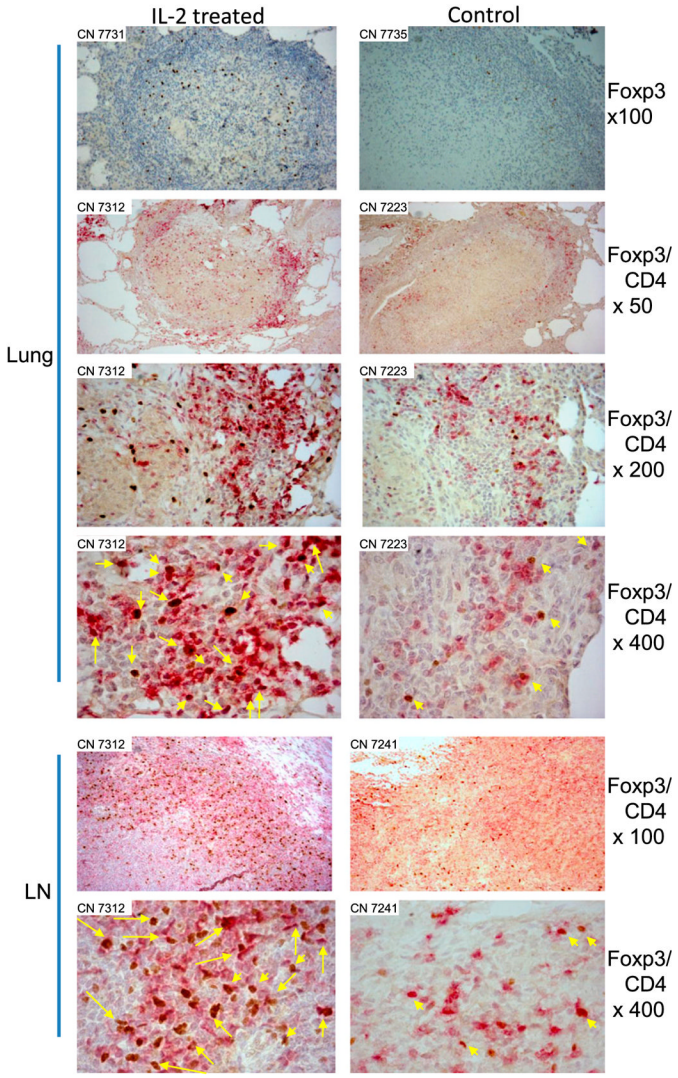

FIGURE 5.

Foxp3^{+}CD4^{+} T cells in lungs and lymph nodes were readily detected in the context of attenuated TB lesions in IL-2–treated macaques. Even at 6 wk after discontinuation of IL-2 treatment, Foxp3^{+}CD4^{+} T cells were readily detectable in granulomatous lung tissues (Lung) and hilar lymph nodes (LN) from IL-2–treated macaques, but less frequently seen from control macaques. Actually, no or few Foxp3^{+} cells were detected in most necrotic TB lesions from the controls. *Top panels*, Single-staining immunohistochemistry analyses of Foxp3, whereas other panels are double-staining analyses of Foxp3 and CD4 (Foxp3/CD4). Macaque ID and image magnification are displayed in *upper left corner* and on *right*, respectively. Foxp3^{+}CD4^{+} T cells are stained as dark red and pointed by yellow arrows in original magnification ×400 image sections (long yellow arrows denote ≥2 Foxp^{+} CD4^{+} cells in the directions or areas); Foxp3^{-} CD4^{+} T cells are stained as purple-red. Similar data were seen for other four IL-2–treated and four control macaques.

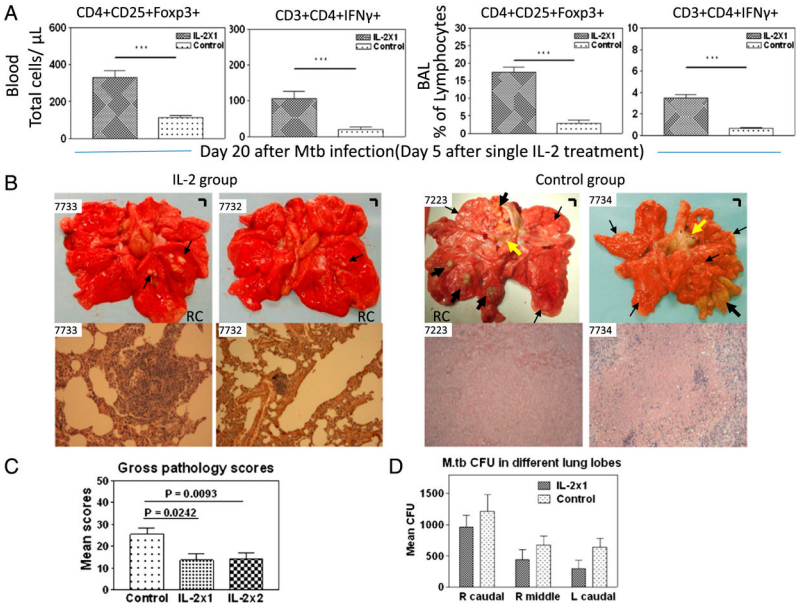

FIGURE 6.

Postinfection IL-2 treatment starting at day 15 after pulmonary *M. tuberculosis* infection also induced increases in Foxp3$^+$ Treg and T effector cells, and conferred resistance to severe TB lesions in four IL-2–treated *M. tuberculosis*-infected macaques. Gross pathology analyses for single IL-2 treatment group were also done at day 65 after *M. tuberculosis* infection. (**A**) Representative data showing IL-2 expansion of Foxp3$^+$ T cells and T effectors at day 5 (peak expansion) after single IL-2 treatment (day 20 after *M. tuberculosis* infection). $n = 4$ for IL-2 group. Major expansion of other CD4$^+$ T, CD8$^+$ T, and γδ T effector cells was also seen in blood and BAL fluid (data not shown). (**B**) Representative gross pathology in cut sections and representative histopathology. Original magnification ×200 for IL-2 group, ×100 for Control group. (**C**) Comparative pathology scores between 1× IL-2–treated, 2× IL-2–treated, and control groups. (**D**) IL-2 treatment, while expanding Treg and T effectors, does not cause Treg-associated increases in *M. tuberculosis* burdens. ***$p < 0.001$.

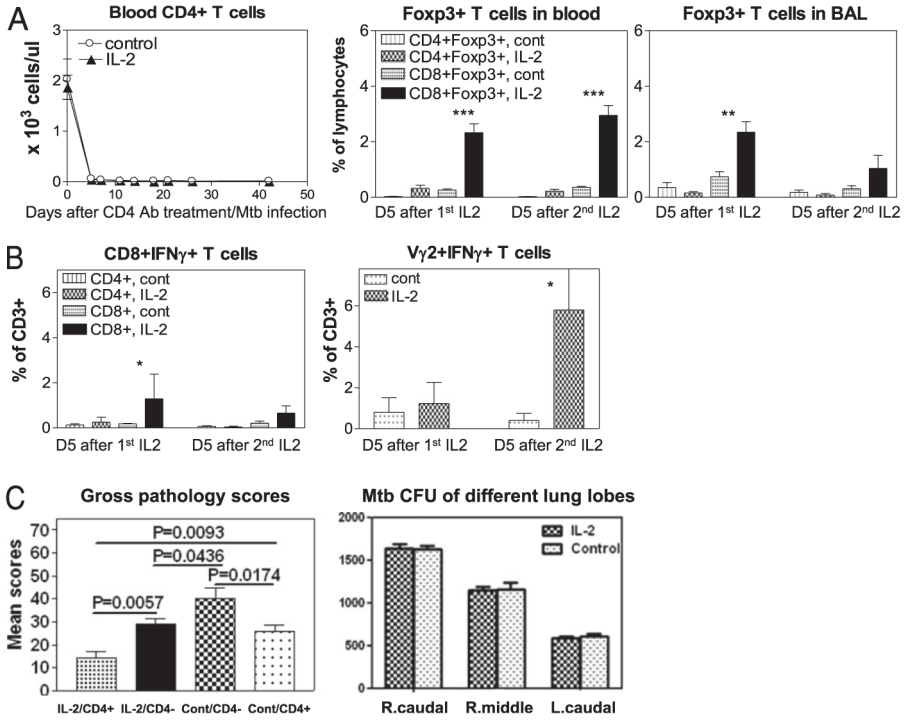

FIGURE 7.

Depletion of IL-2–expanded $CD4^+Foxp3^+$ Treg and $CD4^+$ T effector cells reduced, but did not eliminate, IL-2–induced homeostatic protection against TB lesions. (**A**) A complete in vivo deletion of $CD4^+$ T cells (*left graph*) by anti-CD4 Ab treatment during *M. tuberculosis* infection, and blockage of IL-2 expansion of $CD4^+Foxp3^+$ Treg (*middle* and *right graphs*). Data were collected on day 5 (D5) after the first (1st) and the second (2nd) IL-2 treatment as day 5 after each IL-2 treatment is the peak time for $Foxp3^+$ T cell expansion (see Fig. 1). (**B**) CD4 depletion blocked the ability of IL-2 to expand $CD4^+$ T effectors during *M. tuberculosis* infection. Effector $CD8^+$ T and γδ T cells were detectable. (**C**) *Left graph*, CD4 depletion significantly reduced IL-2–induced resistance to TB lesions (see the first and second bars [from *left*] for comparison between IL-2–treated CD4-depleted [IL-2/$CD4^-$] group and IL-2–treated CD4-not-depleted [IL-2/$CD4^+$] group), but IL-2 treatments still led to detectable resistance to severe TB lesions in the absence of $CD4^+$ T cells (see the second and third bars for comparison between saline-treated [Cont/$CD4^-$] and IL-2–treated [IL-2/$CD4^-$] groups). Another control group, saline-treated CD4-not-depleted (Cont/$CD4^+$) group, was also included for comparison. (C) *Right graph*, No statistical difference in mean *M. tuberculosis* CFU counts from lung lobe homogenates between IL-2–treated CD4-depleted group (IL-2) and control saline-treated CD4-depleted group (Control). Note that extrathoracic TB lesions were seen in the control group, but not in the IL-2–treated group after CD4 depletion. Both IL-2 and control groups of macaques (8 animals) were treated with humanized OKT4A-depleting mAb at a dose of 50 mg/kg on days –5, 10, and 25 after *M. tuberculosis* infection. Intermittent IL-2 treatments, *M. tuberculosis* infection, and evaluations of gross pathology and bacterial burdens were essentially the same as those described above for those macaques without CD4 depletion. The data in this figure are compared between the groups based on our previous observation that control isotype Ab treatment of macaques during *M. tuberculosis* infection does not cause significant depletion or expansion of $CD4^+$ T effector cells, $CD4^+Foxp3^+$ T cells, $CD8^+$ T effector cells, or γδ T effector cells when compared with saline-treated macaques (Ref. 22 and data not shown). $*p < 0.05$, $**p < 0.01$, $***p < 0.001$.